REYNOLDS NUMBER, COMPRESSIBILITY, AND LEADING-EDGE BLUNTNESS EFFECTS ON DELTA-WING AERODYNAMICS

James M. Luckring
NASA Langley Research Center
Hampton, Virginia, U.S.A.

Keywords: *Aerodynamics, Reynolds Number, Compressibility, Vortex Flow, High Angle of Attack*

Abstract

An overview of Reynolds number, compressibility, and leading edge bluntness effects is presented for a 65° delta wing. The results of this study address both attached and vortex-flow aerodynamics and are based upon a unique data set obtained in the NASA-Langley National Transonic Facility (NTF) for i) Reynolds numbers ranging from conventional wind-tunnel to flight values, ii) Mach numbers ranging from subsonic to transonic speeds, and iii) leading-edge bluntness values that span practical slender wing applications. The data were obtained so as to isolate the subject effects and they present many challenges for Computational Fluid Dynamics (CFD) studies.

1 Nomenclature

a,b,c,d	leading-edge contour coefficients, Fig. 3
b/2	wing semispan
C_p	pressure coefficient
$C_{p,le}$	leading-edge pressure coefficient
C_p^*	sonic pressure coefficient
C_0, C_2	modeling coefficients for $C_{p,le}$
c_{bar}	mean aerodynamic chord
c_r	root chord
d	sting diameter
E	Young's modulus
k^+	Inner-law roughness height
M	Mach number
q	dynamic pressure
Rn	Reynolds number based on c_{bar}
r_{le}	streamwise leading-edge radius
t	wing thickness
x, z	body-axis airfoil coordinates
x_m, z_m	leading-edge contour match coordinates
x_v	distance to origin of vortex separation
x/c_r	fraction root chord
α	angle of attack
η	fraction local semispan
Λ	leading-edge sweep

2 Introduction

The delta wing has been a platform for aerodynamic research spanning many decades. One interest in this wing stems from its natural characteristic to generate separation-induced leading-edge vortex flows. These vortex flows are particularly stable when the delta wing is slender, incorporates sharp leading edges, and is oriented at moderate angles of attack.

Interest in delta wing aerodynamics transcends this simple shape, however, since vortex flows can contribute crucial effects to maneuver aerodynamics. Design considerations for high-speed aircraft often result in wings conducive to the formation of separation-induced leading-edge vortices. In some cases these vortex flows have even been exploited such as with the vortex-lift maneuver strakes incorporated into the designs of the F-16 and the F-18 aircraft.

Prediction of vortex flow effects are equally important whether this flow is to be exploited,

tolerated, or avoided. Prediction of aircraft aerodynamics also begs fundamental questions such as scale effects associated with Reynolds number, isolation of effects due to compressibility, and accurate accounting for practical wing design characteristics, such as finite (non-zero) wing leading edge bluntness.

Such practical considerations have spawned the current delta wing research program. With the relatively simple delta wing geometry the fairly complex and relevant flow physics can be studied in greater detail than would be possible on a full aircraft configuration. Whereas early delta wing research focused on the sharp leading-edge case, the present research includes a systematic assessment of leading-edge bluntness effects. This bluntness greatly complicates the aerodynamics of leading-edge vortex flows because the primary leading-edge separation is no longer forced by a sharp leading edge. Reynolds number and angle of attack sensitivities arise that lead to separation onset and progression effects for the blunt leading edge vortex flow that are absent for wings with sharp leading edges.

The author has recently published papers to selectively address Reynolds number and bluntness effects on leading-edge vortex separation at subsonic [1] and transonic [2] speeds. In addition, a paper to address selective compressibility effects [3] has also been published. These analyses are basically transects through an extensive and unique date set [4-7] obtained in the NASA Langley National Transonic Facility. This experimental campaign was designed by this author to isolate Reynolds number and Mach number (compressibility) effects on leading-edge vortex separation for a 65^{o} delta wing with various leading-edge bluntness values. Because the data set is so extensive, the previous publications have only addressed isolated effects. Nonetheless, these papers showed significant Reynolds number, compressibility, and bluntness effects.

In this paper a brief overview and synthesis of these effects is presented. Flow physics considerations will first be discussed with a focus on contrasting sharp and blunt leading-edge vortex flows. The experimental program will next be reviewed followed by selected highlights of the subject aerodynamics.

3 Flow Physics

Early research into separation-induced leading-edge vortices included a focus upon the slender delta wing with sharp leading edges. For such a configuration primary vortex separation is fixed at the sharp leading edge and the origin of the leading edge vortex coincides with the apex of the delta wing. (See Figure 1.) Basic structures and states of this flow are known [8] (secondary vortices, vortex breakdown, etc.) and in the interest of space will not be reviewed. It must be pointed out, however, that many fundamental details of this flow remain unknown and further experimental research to anchor our understanding of the sharp-edged case is warranted [9].

Blunt-edged leading-edge separation is fundamentally more complex because primary separation is no longer affixed at the leading edge. For that matter, the onset of leading-edge vortex separation will be a function of flow conditions and wing geometry. For low to moderate angles of attack the wing could develop fully attached flow. Due to the upwash distribution at the delta wing leading edge the leading edge separation will first occur near the wing tip and then progress up the leading edge with further increase in angle of attack. For an angle-of-attack range the wing will exhibit partial span leading-edge vortex separation with attached flow on the upstream portion of the wing and leading edge vortex separation on the downstream portion. In addition, the separation at any one station will occur near the leading edge but not necessarily precisely at the leading edge such as was the case for the sharp edge. Because the leading-edge separation is now occurring from a smooth surface, the physics of this flow could be quite different from the sharp-edged case.

This added complexity can have considerable impact on the performance and maneuver aerodynamics of slender wings. Strength, position, and the very existence of the

vortex will be affected by leading-edge radius and will change with Mach number, Reynolds number, and angle of attack. While the focus of this work is on steady flows, dynamic effects could also be significantly affected by the blunt leading edge.

4 Experimental Program

The experimental program was conceived to quantify Reynolds number and Mach number effects on separation-induced vortex-flow aerodynamics from a 65° delta wing with blunt leading edges. Some features of the model will first be described followed by a discussion of the experimental facility and the test program.

4.1 Model

The wind tunnel model was designed to generate delta-wing aerodynamics with minimal interference effects. The wing had no twist or camber and had interchangeable leading-edge segments that incorporated the various leading-edge radii. The central portion of the wing was flat. Some basic characteristics of the model are summarized in Figure 2.

The leading-edge contours had a NACA-like polynomial form with a single parameter, the leading edge bluntness. The contours matched the inner flat-plate portion of the wing with continuity through second derivative and hence curvature. This continuity is of course crucial to avoid artificial separation. The bluntness values were selected to be practical as regards values used for maneuvering aircraft.

The emphasis for the experiment was on static surface pressure measurements, and for most configurations there were approximately 183 pressure taps organized along constant percent local semispan locations at constant percent root-chord stations. Pressure taps were also situated directly on the leading edge (i.e., η=1) to facilitate separation onset measurement.

4.2 Facility and Test Program

Experiments were performed in the National Transonic Facility [10] (NTF) at the NASA-Langley Research Center. This tunnel allows for independent control of Mach number (0.1 to 1.2), total pressure (1.2 atm to 8.8 atm), and total temperature (-250 F to 120 F) through the injection of cryogenic nitrogen. The test section is slotted and 8.2 feet square. The NTF has been in operation or approximately 23 years and has supported a fairly broad range of aerodynamic investigations [11] including topics pertinent to military aerodynamics [12].

Through the combination of pressure and cryogenic temperatures the NTF can test at very high Reynolds. In addition, Reynolds number effects, with Mach number and aeroelastics (q/E) held constant, can be measured due to the three degrees of freedom in facility operations (speed, total pressure and total temperature). This feature can be exploited for other means as well, say to vary Mach number while holding Reynolds number and q/E constant. Thus, Reynolds number, Mach number, and aeroelastic effects can be isolated experimentally.

The facility operation envelope for the NTF delta wing along with the range of the delta wing experimental program is shown in Figure 4. The range of test conditions were chosen to be representative of operating conditions for a variety of aircraft incorporating slender-wing flows; cruise conditions for a representative military transport are also shown for reference.

The tests were designed to minimize potential data contaminants including those often referred to as pseudo Reynolds number effects. The wing was hydraulically smooth (k^+<5) for the range of Reynolds numbers investigated. Wing design analysis indicated negligible aeroelastic effects. An offset sting kept the model on the tunnel centerline for the angle-of-attack range investigated. In addition, wind tunnel wall interference was believed to be negligible due to the size of the model relative to the cross sectional area of the slotted-wall test section.

5 Analysis of Results

Results are first presented to contrast the separation-induced vortex flow for a blunt

leading edge with the sharp leading-edge case. This is followed by a discussion of Reynolds number effects for the varying leading-edge bluntness values. Mach number effects are presented next followed by some discussion of the significance of isolating these effects.

5.1 Sharp vs. blunt

Surface pressures for the sharp-edged delta wing show typical separation-induced leading-edge vortex properties, Figure 5. The primary vortex suction peak is situated conically on the wing and diminishes in magnitude as the trailing edge is approached. Outboard of this suction peak turbulent secondary separation is indicated.

Surface pressures for the blunt-edged delta wing clearly demonstrate part span leading-edge vortex separation. See the right side of Figure 5. Attached flow pressures are evident at 20% root chord while leading-edge vortex-like pressures are evident from 60% root chord aft. The origin of the blunt leading-edge vortex for this case is in the vicinity of 30% root chord. The direct comparison of the pressures in Figure 5 at 60% root chord demonstrates the outboard shift of the vortex footprint due to leading-edge bluntness.

The pressures at 60% root chord station also indicate a second suction peak near 60% local semispan. This is inboard of the primary suction peak and may indicate a second co-rotating primary vortex shed from the blunt leading edge.

5.2 Reynolds number effects

The effect of Reynolds number on the blunt leading edge vortex flow is summarized in Figure 6. Results on the left portion of this figure are the same ones used in Figure 5 to compare with sharp-edged flow. Comparison of these results at Rn = 6 million (typical of wind-tunnel conditions) to those at 60 million (representative of flight conditions) show significant recovery of attached flow at the higher Reynolds number. The origin of the leading-edge vortex separation has shifted downstream in association with the higher Reynolds number.

Leading-edge pressures provide a useful means to identify the passage of separation onset (Figure 7). At low angles of attack the leading-edge pressure will follow a trend that can be deduced from attached-flow slender wing theory:

$$C_{p,le} = C_0 - C_2 \sin^2\alpha$$

Analyses of the data [1-3] have demonstrated that this trend is sustained as angle of attack is increased and departure from this trend correlates with separation onset.

The leading-edge pressures can be used to assess the effects of various parameters on leading-edge separation. An example is given in Figure 8. Here Reynolds number is shown to delay separation at three root chord stations. Reynolds number effects occur over a significant angle of attack range at values typical of maneuver conditions. The Reynolds number effects also persist over a greater angle of attack range on the forward portions of the wing.

A summary of leading-edge bluntness effects on the onset and progression of leading-edge separation at low and high Reynolds numbers is presented in Figure 9. At the low Reynolds number the smallest leading-edge bluntness delayed separation onset to approximately 6 degrees angle of attack. Both the medium and the large bluntness values further delayed separation onset. The largest bluntness showed a gradual progression of separation compared to the other two blunt leading edges.

At high Reynolds number separation onset for the small and medium bluntness values has been delayed by about 2 degrees, and separation progression appears to be more gradual. Reynolds number had little effect on the bluntest leading edge.

5.3 Mach number effects

Compressibility effects on leading-edge vortex separation are presented in Figure 10 at the high Reynolds number condition. Results on the left

portion are repeated from previous analysis and exhibit extensive attached flow at Mach number of 0.4. An increase of Mach number to 0.6 has a profound effect on this separation. The 60% root chord station shows well-developed vortex separation and the 40% root chord station also appears to have separated. The origin of leading-edge vortex separation has moved significantly upstream in association with the increase in free stream Mach number from 0.4 to 0.6. This increase in vortex separation with Mach number is also manifested at the low Reynolds number, Figure 11.

The same leading-edge pressure analysis can be used to assess Mach effects for the onset and progression of leading-edge vortex separation. An example is presented in Figure 12 at Rn = 6 million. The data demonstrate that Mach number promotes leading edge separation and that the effects persist for an angle of attack range of approximately 10 degrees at the station shown.

An example of this compressibility effect for the three bluntness values is shown in Figure 13. Data are also included from M = 0.85. At these conditions a decrease in bluntness from the medium to the small value decreased compressibility effects whereas an increase in bluntness to the large value increased compressibility effects.

A summary of Mach effects on the onset and progression of leading-edge separation is presented in Figure 14 for the medium bluntness at Rn = 6 million. Compressibility promotes leading-edge separation over the entire angle of attack range.

5.4 Mach and Reynolds number effects

Results presented in Figure 15 are for Rn = 60 million and constructed similar to those of Figure 13 (Rn = 6 million). At the high Reynolds number the data still demonstrate that Mach number promotes leading-edge vortex separation. However, the separation has been delayed to higher angles of attack as discussed previously. It is noteworthy that the small bluntness leading edge shows significant attached flow and Mach number effects at high Reynolds number (Figure 15) as opposed to low Reynolds number (Figure 13).

A final comparison of these effects is presented in Figure 16 for the medium bluntness wing. The data show, for the onset and progression of leading-edge vortex separation, how Reynolds number delays this phenomena and Mach number promotes it. These effects are comparable in magnitude but opposite in sign. It is vital therefore to isolate these effects for successful prediction to other conditions of interest.

6 Concluding Remarks

Reynolds number, compressibility, and leading edge bluntness effects have been highlighted from a very extensive experimental database on a 65° delta wing. The particular data set is fairly unique in that Reynolds number and Mach number effects have been isolated. Emphasis has been placed on the onset and progression of leading-edge vortex separation for the delta wing with various values of leading edge bluntness.

An increase in Reynolds number, with Mach number held constant, was demonstrated to delay the onset of leading-edge vortex separation. Conversely, and increase in Mach number, with Reynolds number held constant, was demonstrated to promote leading-edge vortex separation. These effects of Mach and Reynolds number can be comparable in magnitude but opposite in sign and were shown to be significant at angles of attack representative of maneuver conditions. It appears to be vital therefore to isolate Mach and Reynolds number effects. In addition, leading-edge bluntness was demonstrated to modulate these effects. The data present many challenging opportunities to assess CFD simulation capability to predict blunt leading-edge vortex flow aerodynamics.

7 References

[1] Luckring J M. Reynolds Number and Leading-Edge Bluntness Effects on a 65° Delta Wing. AIAA Paper 2002-0419, January 2002.

[2] Luckring J M. Transonic Reynolds Number and Leading-Edge Bluntness Effects on a 65° Delta Wing. AIAA Paper 2003-0753, January 2003.

[3] Luckring J M. Compressibility and Leading-Edge Bluntness Effects on a 65° Delta Wing. AIAA Paper 2004-765, January 2004.

[4] Chu J, and Luckring J M. Experimental Surface Pressure Data Obtained on 65° Delta Wing Across Reynolds Number and Mach Number Ranges. Volume 1 – Sharp Leading Edge, *NASA TM-4645*, February 1996.

[5] Chu J, and Luckring J M. Experimental Surface Pressure Data Obtained on 65° Delta Wing Across Reynolds Number and Mach Number Ranges. Volume 2 – Small Leading Edge, *NASA TM-4645*, February 1996.

[6] Chu J, and Luckring J M. Experimental Surface Pressure Data Obtained on 65° Delta Wing Across Reynolds Number and Mach Number Ranges. Volume 3 – Medium Leading Edge, *NASA TM-4645*, February 1996.

[7] Chu J, and Luckring J M. Experimental Surface Pressure Data Obtained on 65° Delta Wing Across Reynolds Number and Mach Number Ranges. Volume 4 – Large Leading Edge, *NASA TM-4645*, February 1996.

[8] Hummel D. On the Vortex Formation Over a Slender Wing at Large Incidence, *AGARD CP-247*, Paper No. 15, January 1979.

[9] Hummel D. and Redeker G. A New Vortex Flow Experiment for Computer Code Validation. *RTO MP-069*, Paper No. 9, March 2003.

[10] Fuller D E. Guide for Users of the National Transonic Facility, *NASA TM-83124*, 1981.

[11] Wahls R A. The National Transonic Facility – A Research Retrospective, AIAA Paper 01-0754, January 2001.

[12] Luckring J M. An Overview of National Transonic Facility Investigations for High Performance Military Aerodynamics, AIAA Paper 01-0906, January 2001.

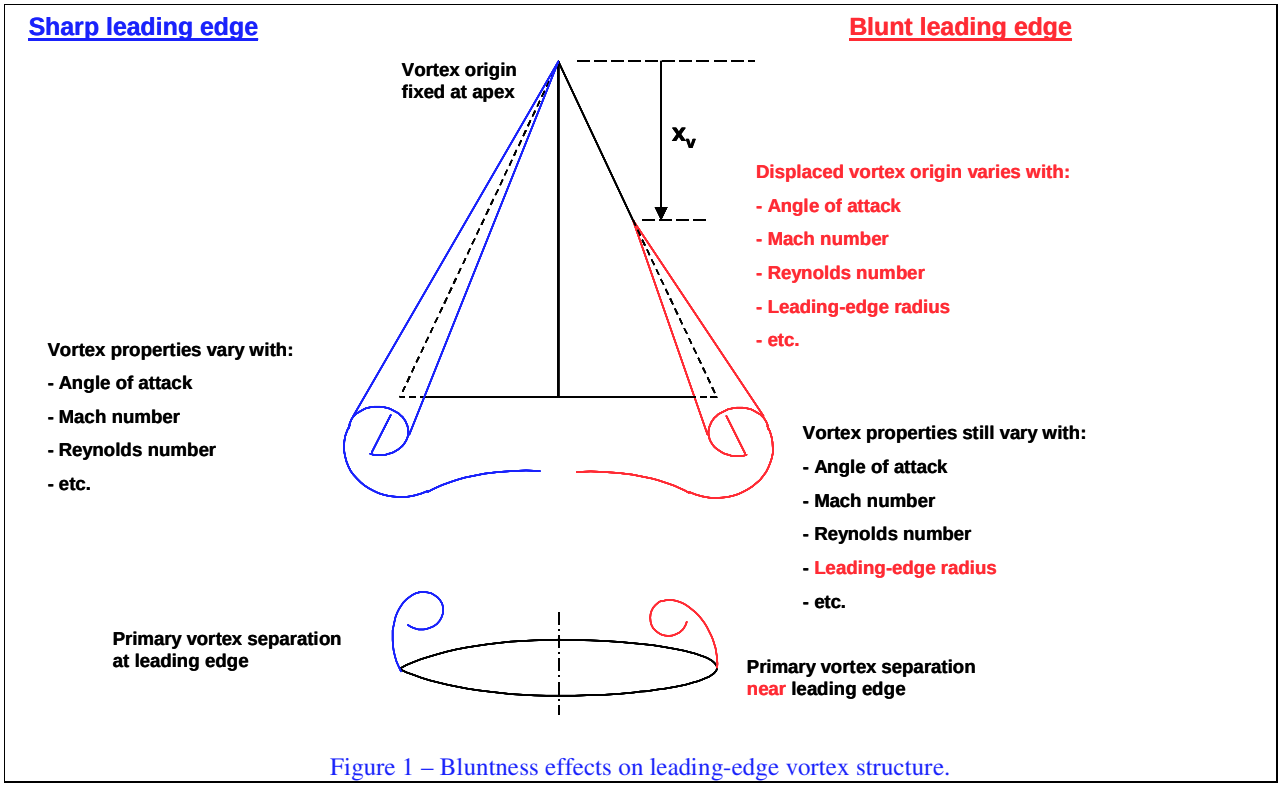

Figure 1 – Bluntness effects on leading-edge vortex structure.

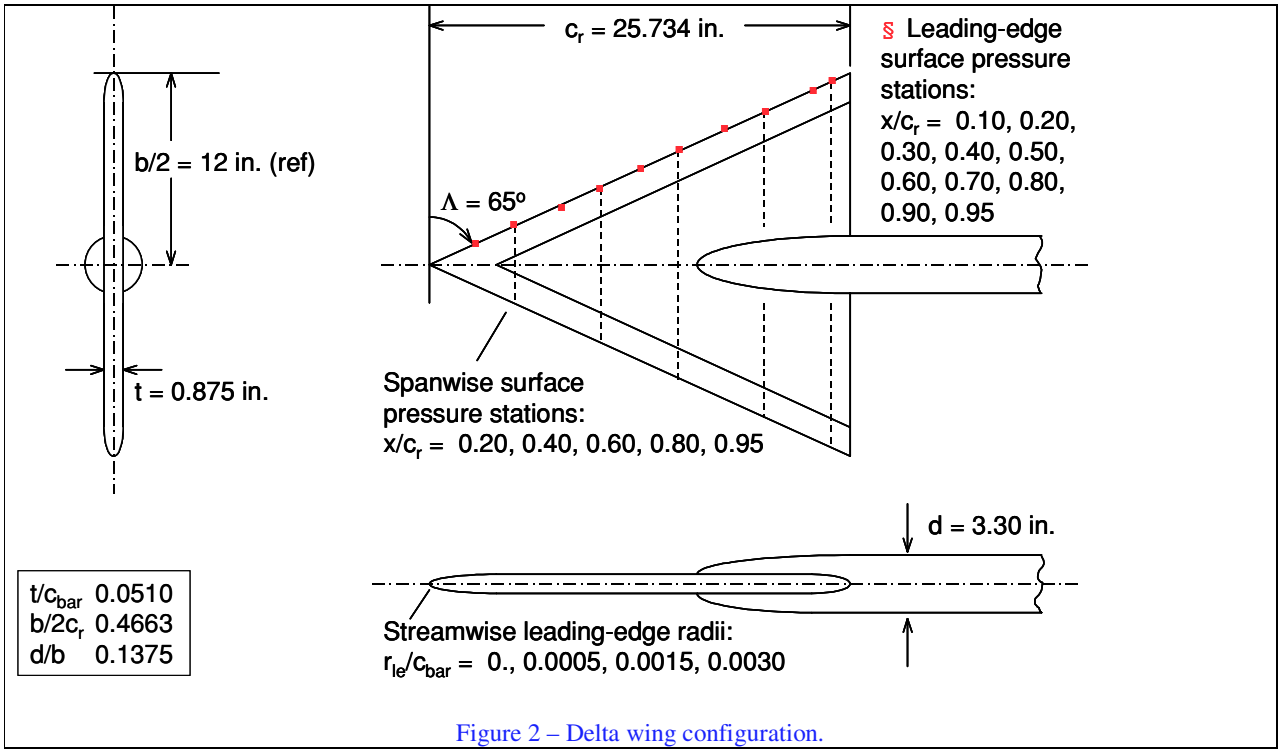

Figure 2 – Delta wing configuration.

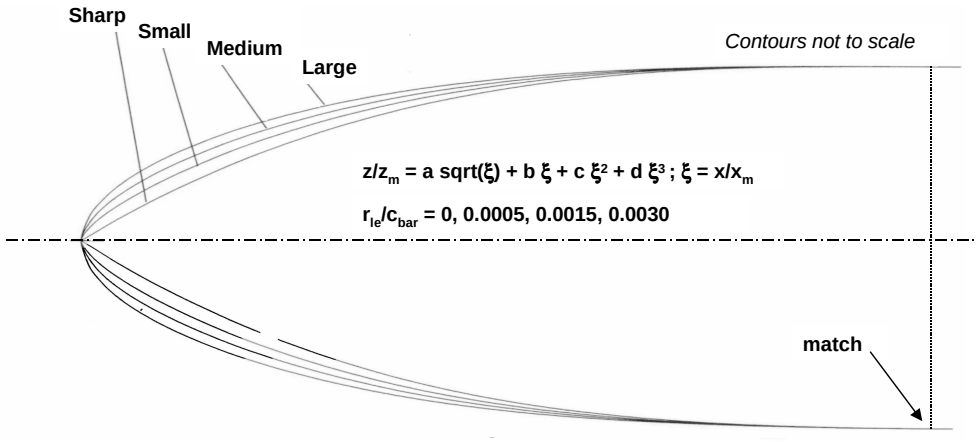

Figure 3 – Streamwise leading-edge contours for NTF delta wing.

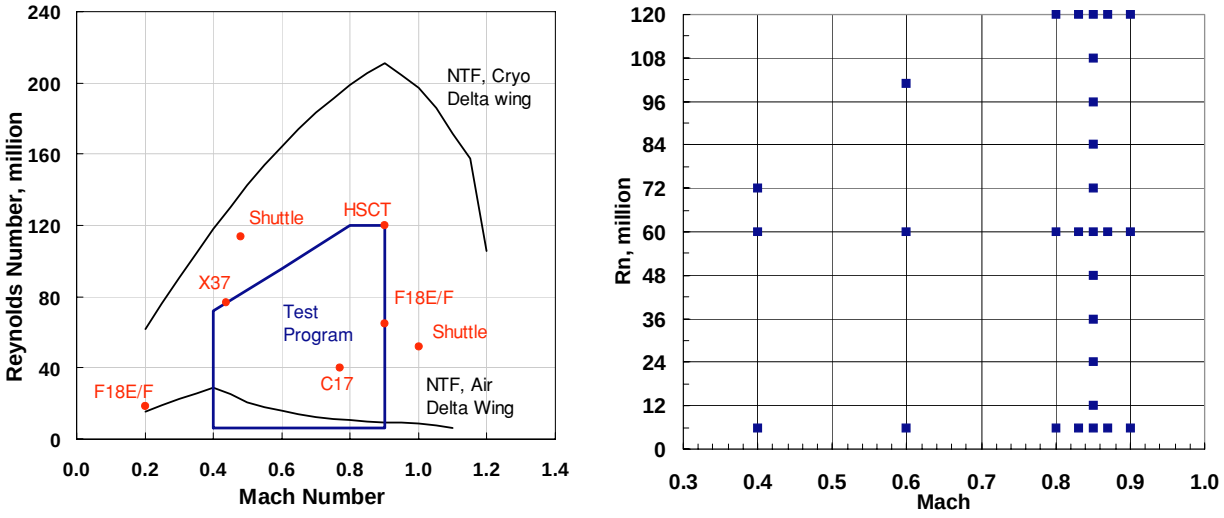

a) NTF envelopes and aircraft operating conditions. b) Representative delta-wing test matrix.

Figure 4 – Reynolds number and Mach number conditions.

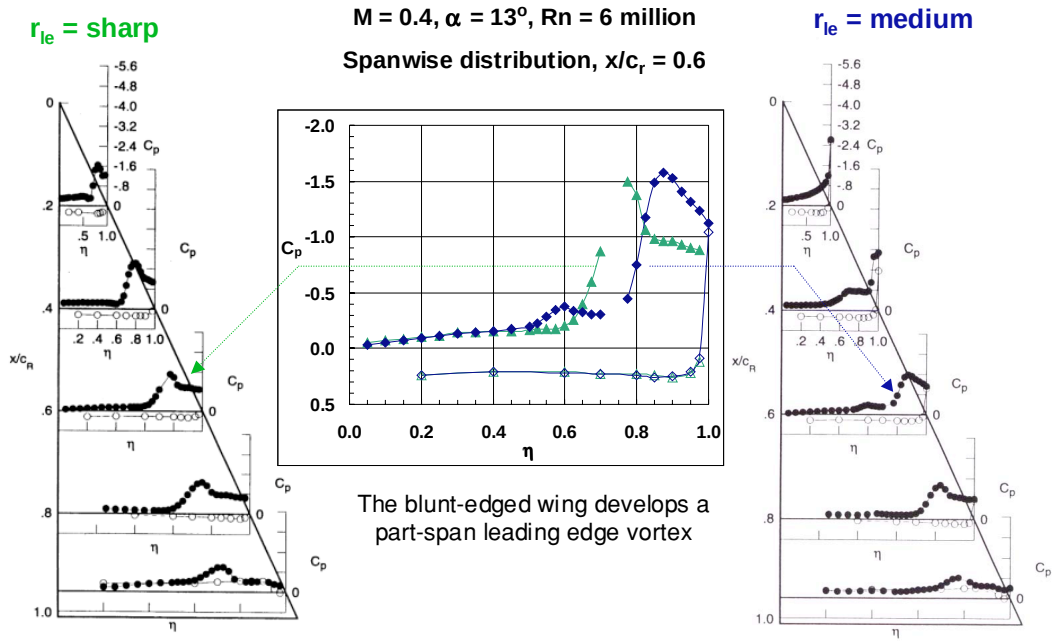

Figure 5 – Leading-edge bluntness effect on surface pressures.

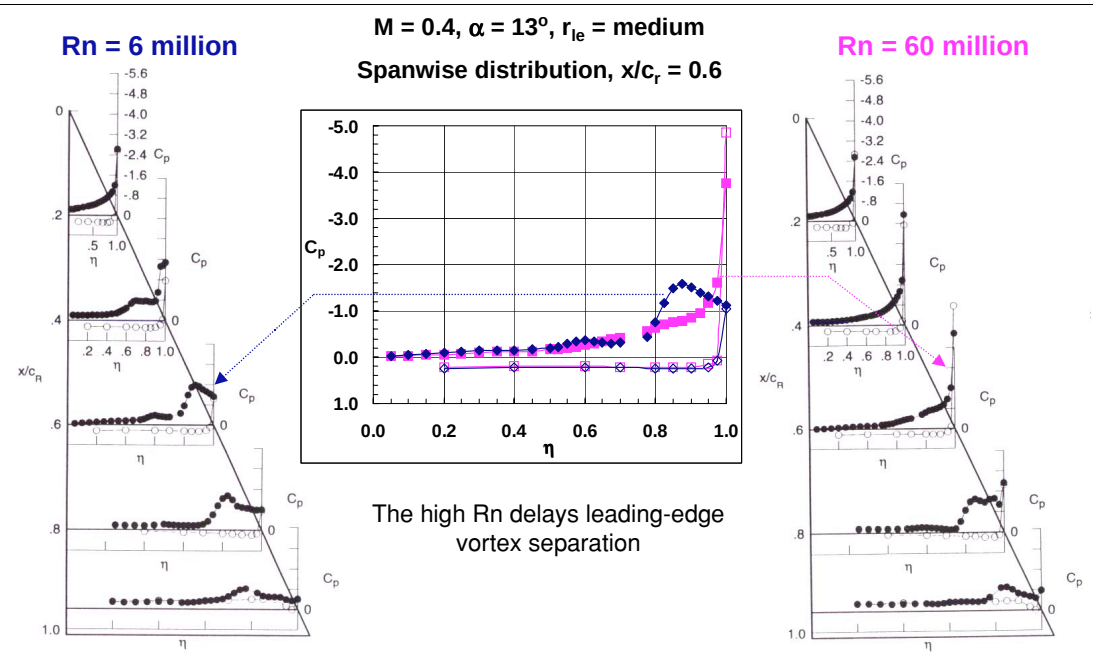

Figure 6 – Reynolds number effect on blunt leading-edge separation.

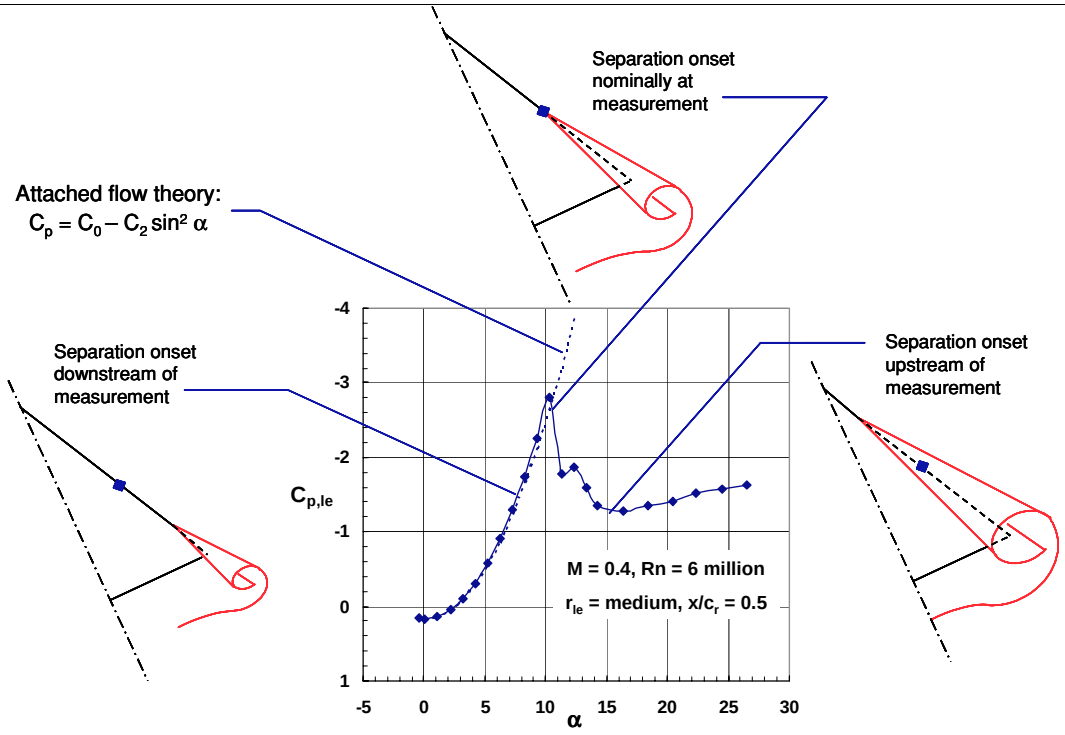

Figure 7 – Correlation of separation onset with leading-edge pressure distribution.

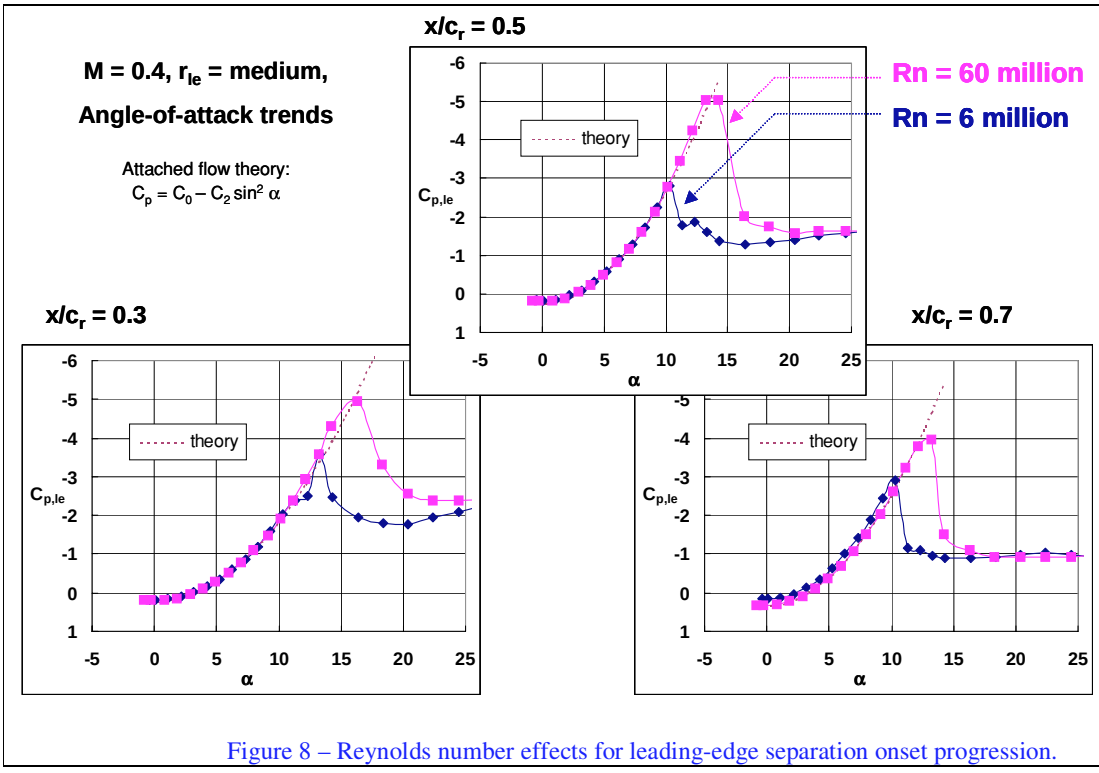

Figure 8 – Reynolds number effects for leading-edge separation onset progression.

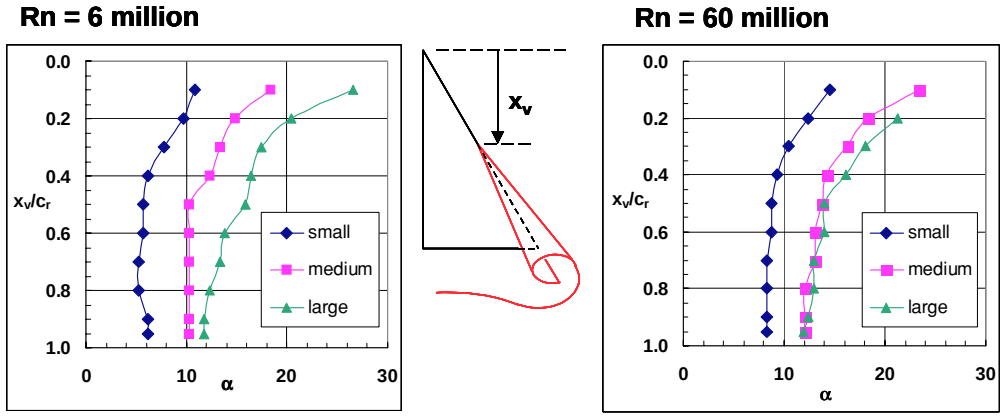

- Small and medium bluntness
  - Fairly rapid progression of separation
  - About a 4° offset between them
- Large bluntness
  - More gradual separation progression

- Small and medium bluntness
  - More gradual separation progression
  - About a 2° offset from Rn = 6 million
- Large bluntness
  - Little Reynolds number effect

Figure 9 – Bluntness effect on separation onset progression at low and high Reynolds number. M=0.4

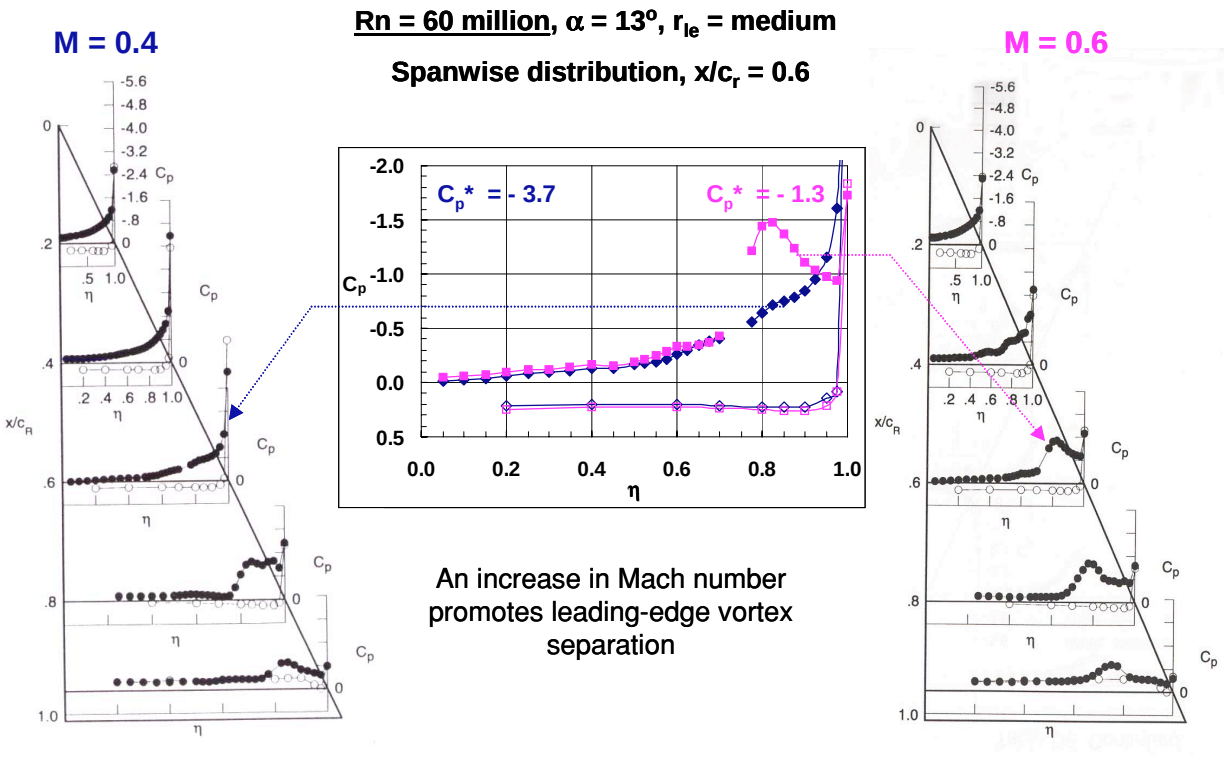

Figure 10 – Compressibility effect on blunt leading-edge separation – high Reynolds number

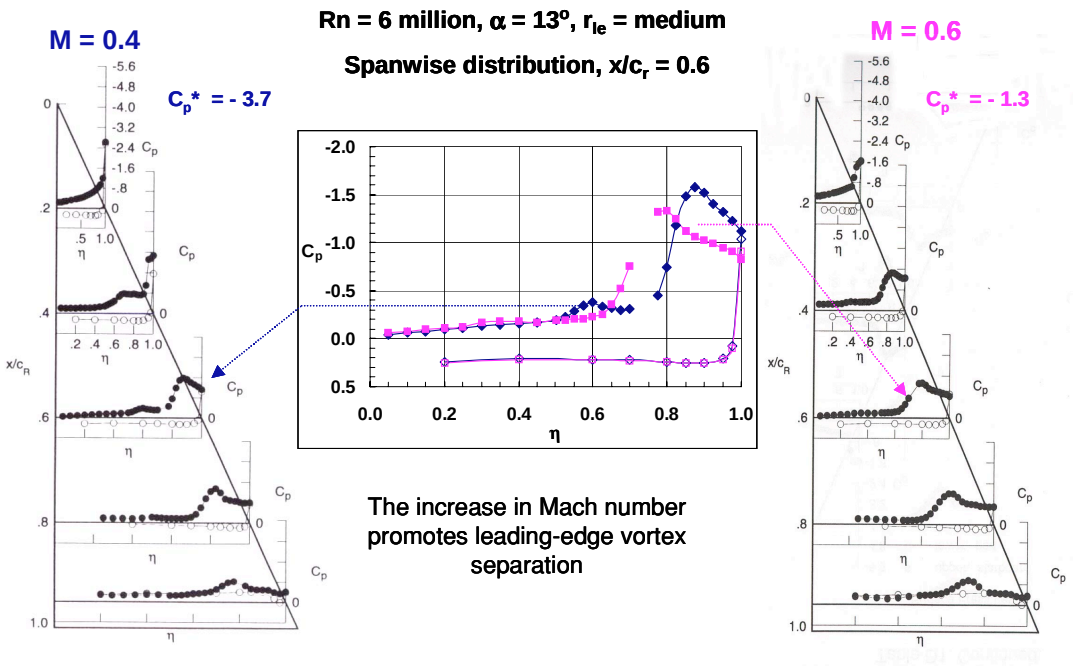

Figure 11 – Compressibility effect on blunt leading-edge separation – low Reynolds number.

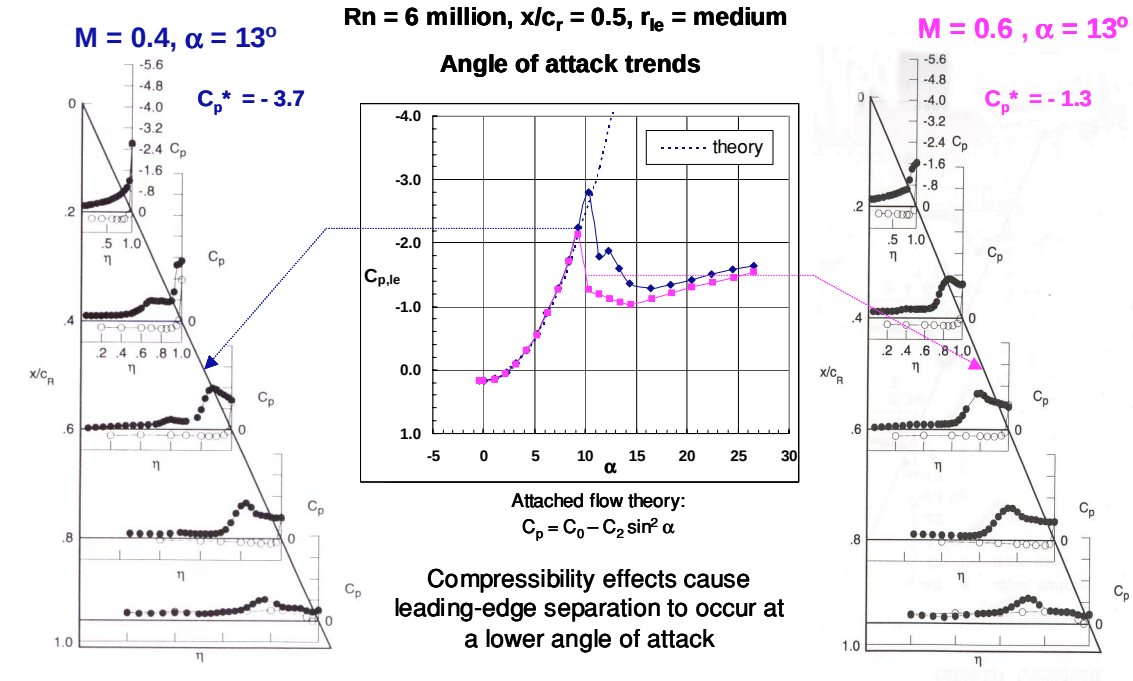

Figure 12 – Compressibility effect on blunt leading-edge pressures.

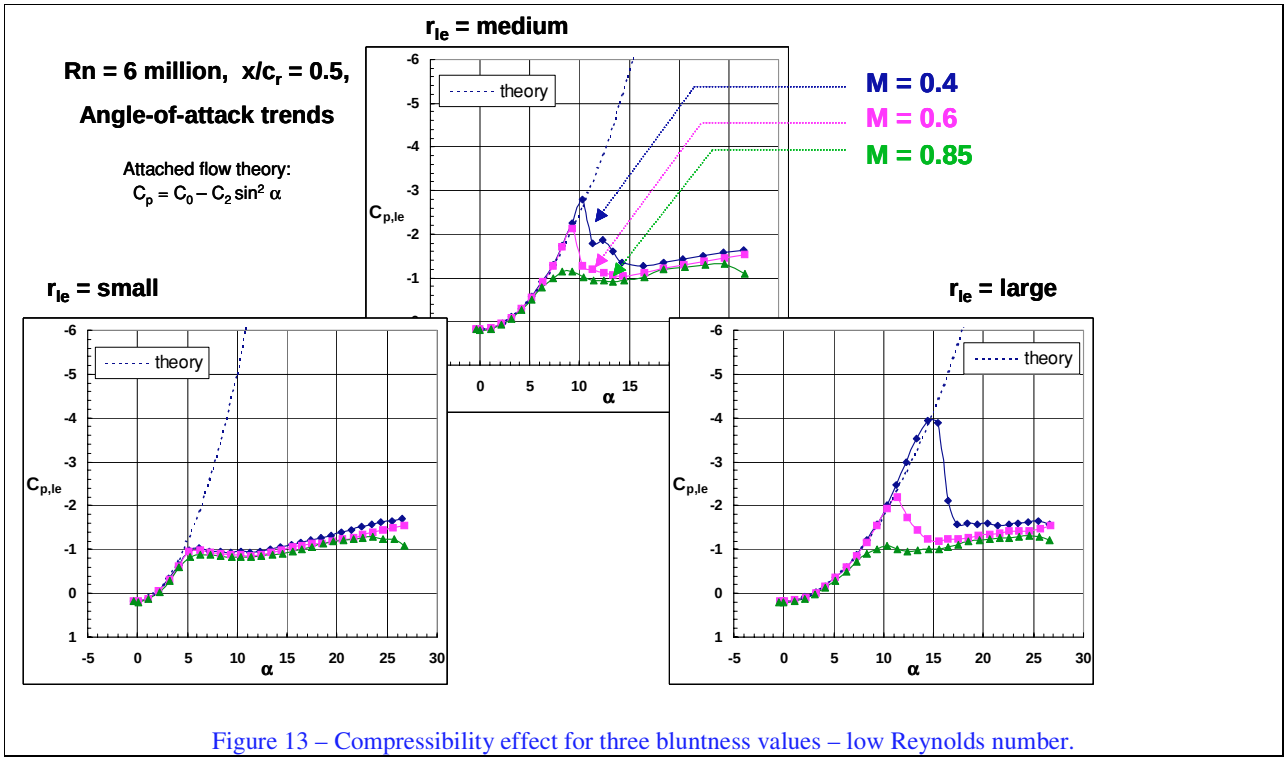

Figure 13 – Compressibility effect for three bluntness values – low Reynolds number.

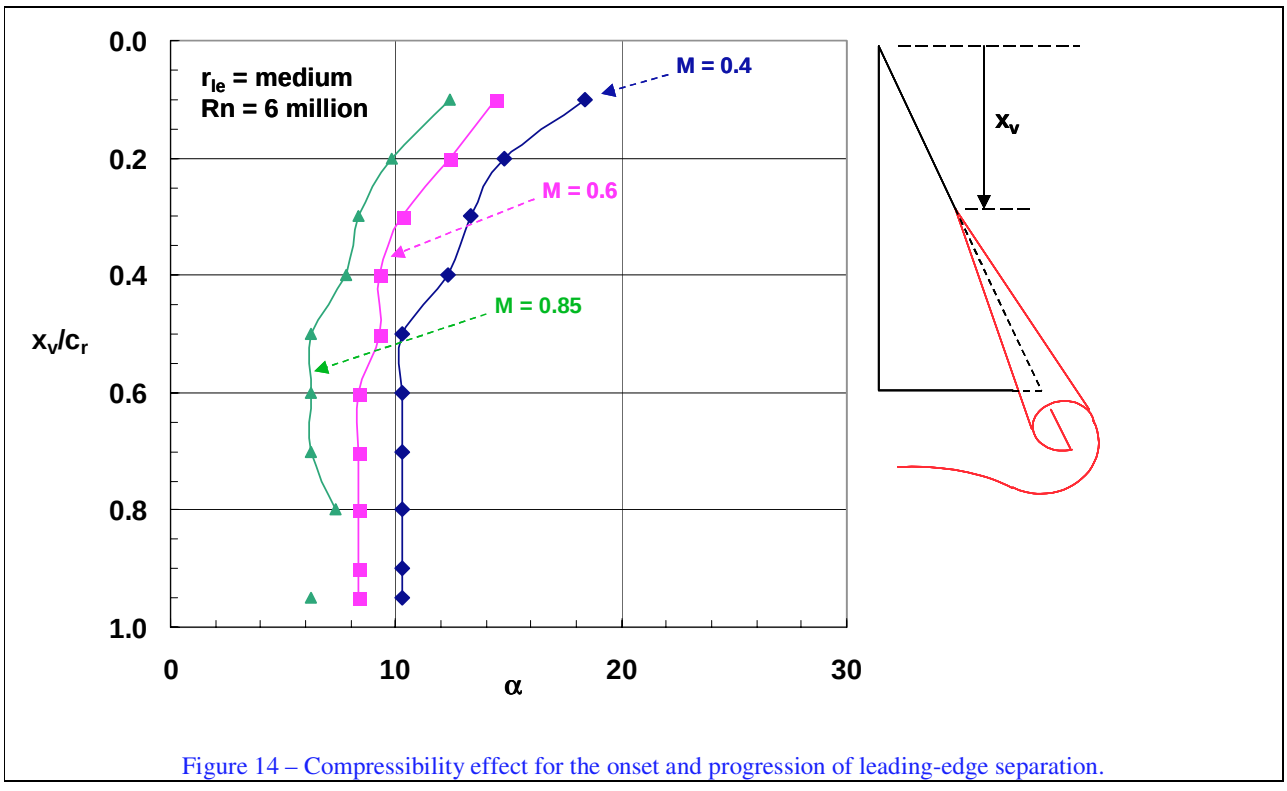

Figure 14 – Compressibility effect for the onset and progression of leading-edge separation.

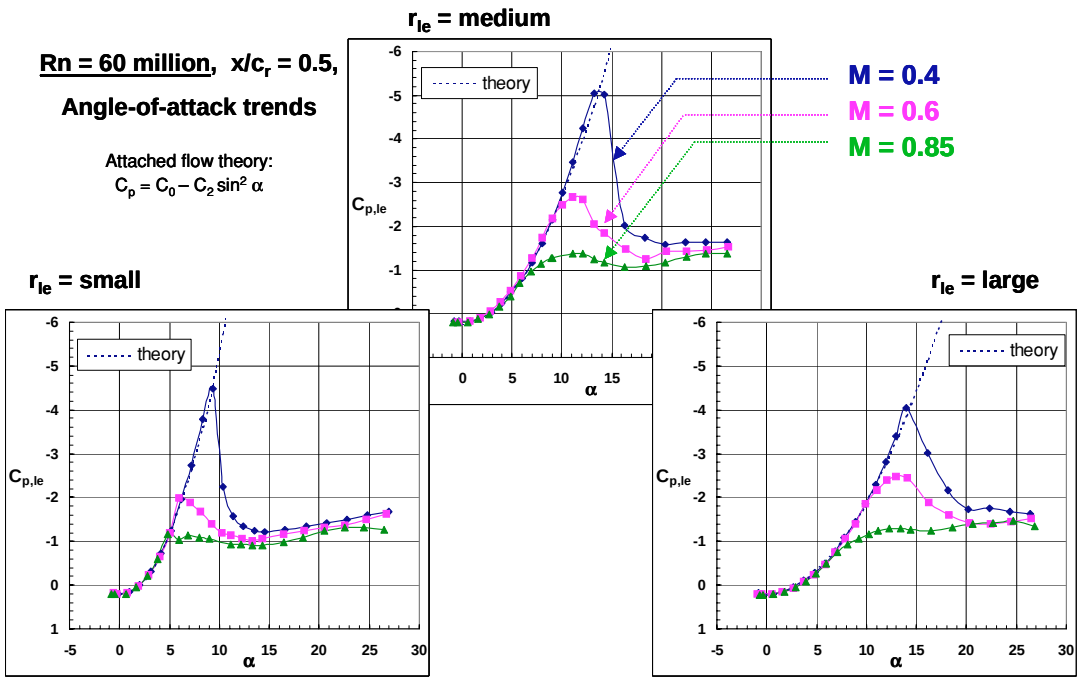

Figure 15 – Compressibility effect for three bluntness values – high Reynolds number.

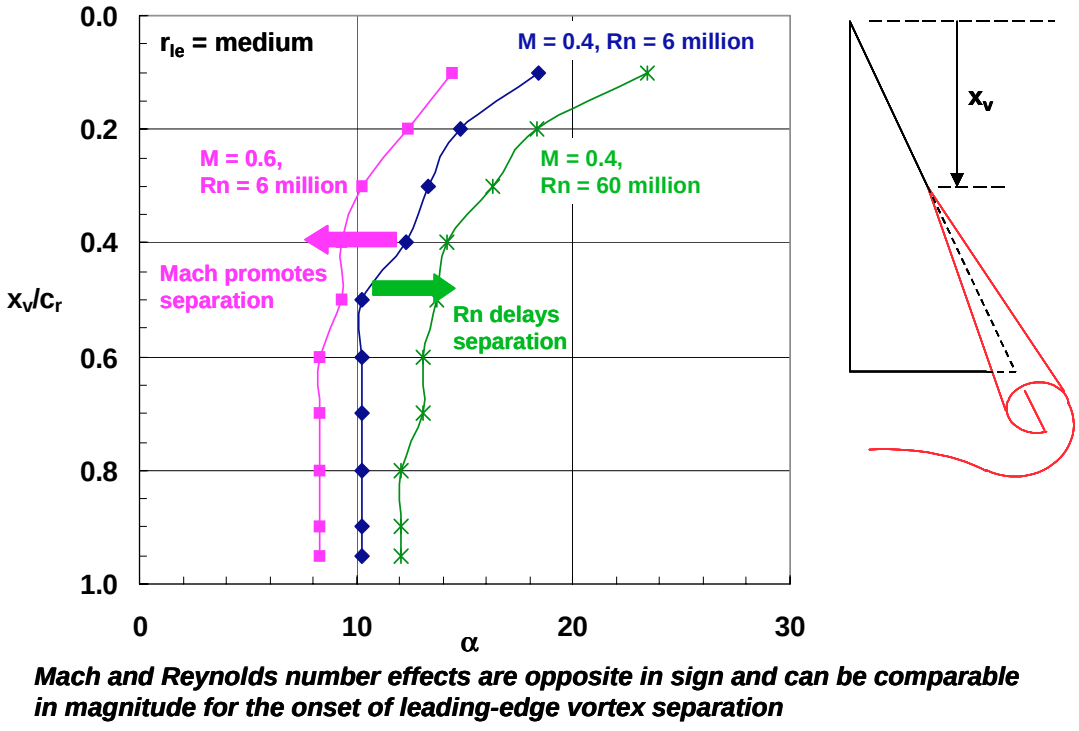

Figure 16 – Mach and Reynolds number effects for the onset and progression of leading-edge separation.